

Electron magnetic resonance in lithium oxide from a centre containing Fe^{3+}

This article has been downloaded from IOPscience. Please scroll down to see the full text article.

1991 J. Phys.: Condens. Matter 3 8467

(<http://iopscience.iop.org/0953-8984/3/43/013>)

View [the table of contents for this issue](#), or go to the [journal homepage](#) for more

Download details:

IP Address: 171.66.16.159

The article was downloaded on 12/05/2010 at 10:38

Please note that [terms and conditions apply](#).

Electron magnetic resonance in lithium oxide from a centre containing Fe^{3+}

J M Baker, A A Jenkins and R C C Ward
Clarendon Laboratory, Parks Road, Oxford OX1 3PU, UK

Received 14 June 1991

Abstract. EPR has been performed on single crystals of nominally pure ${}^7\text{Li}_2\text{O}$: (a) as grown, (b) after x-irradiation, and (c) after subsequent annealing. (a) shows evidence of several sites of Fe^{3+} in low abundance; (b) shows additional spectra from an electron centre with $g = 2.003(1)$, associated with a brown coloration of the crystal, and also from Fe^{3+} at tetragonal sites; (c) shows that the electron centre (and the coloration) has been destroyed and the tetragonal Fe^{3+} concentration has been greatly enhanced. The fine structure parameters of the tetragonal Fe^{3+} centres, $b_2^0 = -0.1445(5) \text{ cm}^{-1}$, $b_4^0 = -27(3) \times 10^{-4} \text{ cm}^{-1}$ and $b_4^2 = -90(2) \times 10^{-4} \text{ cm}^{-1}$, are shown to be well described by the Newman superposition model, using a structural model for the centre comprising Fe^{3+} substituting for Li^+ and two adjacent Li^+ vacancies. Models are proposed for the changes that occur in this material on x-irradiation and annealing.

1. Introduction

Lithium oxide, Li_2O , has potential application as a blanket material for nuclear fusion reactors, where its role would be to convert energetic neutrons into useful heat, and to breed tritium for the fusion reaction. It also has potential for use in batteries as a Li^+ conducting electrode. Li_2O crystallizes in the cubic antifluorite structure, i.e. it has the same structure as CaF_2 with anions and cations interchanged (the Li^+ ions form a simple cubic array and the O^{2-} ions occupy alternate cube centres; see figure 2). Li_2O exhibits thermally induced dynamic Frenkel disorder and fast-ion conduction at high temperatures, in analogy with that shown by the anions in compounds with the fluorite structure (Farley *et al* 1988, Ohno *et al* 1979).

With regard to the defect properties of Li_2O , it is of interest to study defects in the antifluorite structure produced by impurities, particle irradiation or optical excitation, for comparison with the extensive literature on such defects in fluorite hosts. It is also interesting to compare such defects with those in other oxides such as MgO , Si_2O and Al_2O_3 .

In this paper we report various sorts of magnetic resonance measurements in single crystals of nominally pure ${}^7\text{Li}_2\text{O}$, such as ODMR and EPR in the crystals as grown, and after various types of irradiation and thermal treatment.

2. Crystal growth

The preparation and crystal growth of Li_2O are complicated by problems of volatility and dissociation, the chemical reactivity of both Li_2O and Li metal, and the high

temperature involved (melting point 1705 K). Lithium oxide, unlike lithium metal, is compatible with platinum, but the temperatures involved are very high for the use of Pt crucibles. However, it has proved possible to grow single crystals of Li_2O from the melt by the Bridgman-Stockbarger technique using a closed platinum crucible supported by an outer alumina crucible. Previously, the only growth methods used for Li_2O have been the floating zone method heated by IR imaging (Shindo *et al* 1979) or a vacuum fusion method (Akiyama *et al* 1980).

The Li_2O was prepared by the vacuum decomposition of the carbonate, Li_2CO_3 , which is stable in air at room temperature, by heating to 900 °C in a platinum boat inside a continuously evacuated silica tube furnace. All handling of the powder starting material was thereafter carried out in an inert gas glovebox (in single crystal form, Li_2O was found to react only slowly with laboratory air, enabling x-ray orientation and room temperature measurements to be carried out without need for encapsulation). Crystal growth was undertaken in a Stockbarger furnace heated by RF induction with the coil mounted externally around the double-walled, water-cooled silica furnace tube assembly. The furnace could be evacuated ($< 10^{-6}$ mbar) and was backfilled with 1.2 bar purified argon for the growth. The Li_2O was contained in a Pt crucible with a close-fitting lid, which together with the Ar overpressure was sufficient to prevent excessive decomposition or volatilization. For crystal growth the Pt/alumina crucible assembly was translated at a speed 1–2 mm hr⁻¹ (in our design the complete furnace assembly is translated vertically out of the stationary RF coil).

Since the crystals were grown originally for neutron scattering studies of lattice dynamics (Farley *et al* 1988), starting material enriched in ⁷Li isotope was used in order to avoid the high neutron absorption exhibited by ⁶Li. The absolute purity of the ⁷Li₂CO₃ starting material is not known, and could limit the quality of the crystals grown. However, the effects of a limited degree of decomposition and oxygen loss are probably more significant. The solidified cylindrical charge was always found to be segmented into a number of individual crystals, each typically 15 × 5 × 1–3 mm in size. They were transparent and colourless. For the magnetic resonance experiments the crystals were oriented and cut into cubes with {100} faces of 2 mm on an edge.

3. Electron paramagnetic resonance

EPR at about 35 GHz and at room temperature in the crystals as grown exhibited a complicated spectrum of weak lines of similar but not equal intensity, covering a wide range of magnetic fields. This spectrum was very anisotropic and, even though the line width was quite small (~ 13 gauss), the lines were too weak, and their angular variation too complicated for it to be easily measured. The lines appeared to fall into groups, each of which moved approximately as a group, but the relative intensities of those in a group and their spacing and their relative angular variation, indicated that they are not a group of hyperfine lines. In hindsight, after analysis of the spectra to be described below, it is likely that they arise from Fe³⁺ in sites which are broadly similar, but differ in detail. The concentration of these sites is probably a few ppm.

The EPR at 4.2 K, showing the same spectrum and no additional lines, was heavily saturated, indicating that the spin-lattice relaxation time is very long, as one might expect for an S-state ion.

Irradiation with x-rays for 5 hours at room temperature using 60 kV x-rays from a Matchlett OEG-60 tube running at 60 mA, produced a brown coloration of the

crystal. The EPR at room temperature showed no change in the complex spectrum of lines observed in the crystal as grown, but in addition it exhibited two new rather more intense spectra. The first was a single isotropic line with $g = 2.003(1)$ and a line width of about 13 gauss. The second was a set of three equivalent anisotropic spectra with fourfold rotational symmetry about the three (100) directions. Each spectrum comprises five lines, corresponding to $S = 5/2$, without hyperfine structure, and so presumably due to Fe^{3+} at tetragonal sites. The spectrum was interpreted using the spin-Hamiltonian:

$$H = g^{\parallel} \mu_B B_z S_z + g^{\perp} \mu_B (B_x S_x + B_y S_y) + B_2^0 O_2^0(S) + B_4^0 O_4^0(S) + B_4^4 O_4^4(S)$$

where the spin operators $O_n^m(S)$ are defined by Stevens (1952). The terms in B_4^0 and B_4^4 are much smaller than that in B_2^0 , and are therefore determined much less precisely. The effect of B_4^4 is most clearly seen as a small angular variation in the perpendicular plane with four-fold symmetry about the z -axis. The spin-Hamiltonian parameters which give the best fit to the data are given in table 1 in terms of the more usual parameters:

$$b_2^0 = 3B_2^0 \quad b_4^0 = 60B_4^0 \quad b_4^4 = 60B_4^4.$$

This spectrum also had a line width of about 13 gauss which was the same for all lines. The line width arises presumably from unresolved transferred hyperfine structure from neighbouring 7Li nuclei.

Table 1. Spin-Hamiltonian parameters for Fe^{3+} .

g	2.008(2)
b_2^0	$-1445(5) \times 10^{-4} \text{ cm}^{-1}$
b_4^0	$-27(3) \times 10^{-4} \text{ cm}^{-1}$
b_4^4	$-90(2) \times 10^{-4} \text{ cm}^{-1}$
b_4^4/b_4^0	3.3(4)

The lines of the two spectra were of similar intensity suggesting, as the Fe^{3+} spectrum comprises 15 lines, that the concentration of Fe^{3+} is an order of magnitude greater than the centre at $g = 2.003$. The spectrum at 77 K was the same as at room temperature, and that at 4.2 K was heavily saturated, but showed no new lines. X-irradiation at 77 K or at 4.2 K, followed by measurement at these temperatures without warming the sample, produced the same spectrum as x-irradiation at room temperature.

It proved very difficult to make a clear determination of the absolute sign of b_2^0 by measuring the relative intensities of the lines as a function of temperature. At room temperature, all lines had about the same width, but the relative intensities of fine structure lines were weaker than expected towards the outer edges of the spectrum, though symmetrical about the centre. At 4 K, the spectrum was very heavily saturated, with no obvious pattern to the relative line strength, suggesting that different relaxation rates played a greater role than population differences. At 40 K, the lines appeared to be unsaturated, but differences in the relative intensities of the lines between 40 K and 300 K were not consistent between spectra from differently oriented

sites; nor did they correlate well with the Boltzmann factor, so there may still have been incipient saturation at 40 K. However, within the spectrum with B parallel to the tetragonal axis the relative intensities are consistent, and indicate negative b_2^0 , so we conclude that this is the more likely sign.

Heating the irradiated crystal to 500 °C for 2 hours in air made no difference to the complicated spectrum in the crystal as grown, but it (a) destroyed the signal from the centre at $g = 2.003$, (b) increased the signal/noise ratio of the tetragonal Fe^{3+} spectrum by an order of magnitude to a concentration of 30–100 ppm, (c) removed the brown coloration, and (d) increased the weight of the crystal by 1 to 2% and produced a white surface layer. Re-irradiation with x-rays again produced the brown coloration, but no further change in the spectrum of Fe^{3+} .

The weak complicated spectrum in the crystal as grown appears to be grouped around, and to follow approximately, the angular variation of the tetragonal Fe^{3+} spectrum, which suggests that it arises from a similar site, but distorted by association with a variety of defects which change it in slightly different ways. Similar sets of slightly distorted sites were reported by Baker and Chaplin (1970) in SrF_2 and BaF_2 containing Ce^{3+} and by Baker and Robinson (1983) in quartz associated with a defect thought to be O_2^- .

4. ODMR experiments

Irradiation of the sample at 1.5 K with x-rays from a Matchlett OEG-60 tube operating at 50 keV and 40 mA produced a luminescence in the visible region. The intensity of this luminescence detected by an EMI 9789Q photomultiplier (200–600 nm response), decreased steadily as an applied magnetic field was increased from 0 to 5 T, suggesting the involvement of paramagnetic centres in the luminescence process. These measurements were made with the sample in a microwave cavity, so that a search could be made for ODMR by detecting the changes in luminescence produced by simultaneous excitation with up to 1.2 W of microwaves at 24 GHz incident on the cavity. However, no ODMR signals were detected, either without modulation, or using amplitude modulation of the microwave power and phase sensitive detection at audio-frequencies down to 2 Hz.

5. Optical absorption measurements

Figure 1 shows the absorption of electromagnetic waves from 185 to 860 nm of a parallel-sided specimen of about 1 mm thickness with polished surfaces. This shows no indication of the UV absorption edge, indicating that the band gap is greater than 7 eV.

The spectrum is shown for the crystal as grown (a), after x-irradiation (b), after heating (c) and after further x-irradiation (d). The small differences between (b) and (d) are probably not significant, suggesting that after the first irradiation, the effects of x-irradiation and annealing are reversible. The reversible creation by x-irradiation of the strong absorption in the blue and near UV, which causes the visible coloration of the crystal, appears to be correlated with the creation of the centre at $g = 2.003$, but we have no evidence of direct correspondence. However, some irreversible change occurs on first irradiation of the crystal as grown, as the strong absorption in the UV which is apparent in spectrum 1(a) is not present in spectrum 1(c).

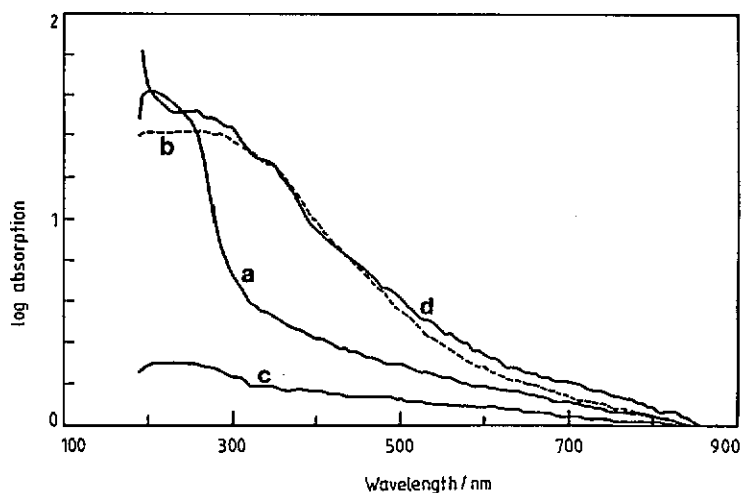


Figure 1. Absorption spectrum of Li_2O : (a) as grown, (b) after irradiation with 60 keV x-rays for 5 hours, (c) after subsequent heating in air for 2 hours at 500 °C, (d) after re-irradiation with x-rays.

6. Models of the site of Fe^{3+}

In this section we consider possible models for the Fe^{3+} site. Figure 2 shows the crystal structure of Li_2O , for which $a_0 = 0.4619$ nm. It seems most likely that Fe^{3+} would substitute for a Li^+ ion.

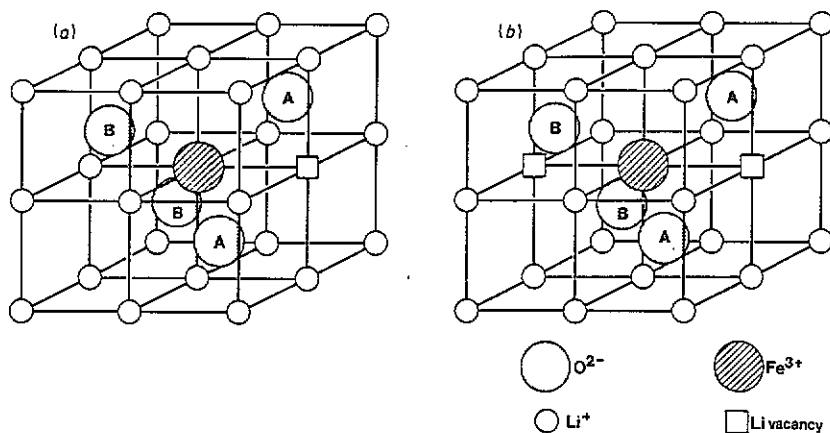


Figure 2. (a) The unit cell of Li_2O , a_0 on a side, showing possible substitutional sites for Fe^{3+} . (b) The structure of Li_2O is obtained by replacing Fe^{3+} and Li vacancies by Li^+ ions.

We briefly wish to examine an alternative possibility that Fe^{3+} occupies one of the vacant interstitial sites at the centre of a cube of Li^+ ions, such as that in the lower left hand corner of figure 2, but it is difficult to envisage how the extra $+3e$ of charge could be completely compensated in such a way as to produce a site of tetragonal symmetry. Possibilities for partial charge compensation are: (i) one interstitial O^{2-}

in the vacant site distant a_0 along [100], and possibly a second O^{2-} in the vacant site distant a_0 along $[\bar{1}00]$, or (ii) four Li^+ vacancies in one face of the cube of Li^+ surrounding the Fe^{3+} .

As both of these seem improbable, we examine how the extra charge on Fe^{3+} at a substitutional site for Li^+ could be compensated to produce a site of tetragonal symmetry. A single Li^+ vacancy distant $a_0/2$ along [100] would not produce the required symmetry, as the two O^{2-} ligands of Fe^{3+} which are also neighbours of the vacancy (labelled A in figure 2(a)) would change their positions differently from the two ligands (labelled B) on the other side of Fe^{3+} , leaving Fe^{3+} at a site of C_{2v} symmetry. The same site symmetry would be produced if the Fe^{3+} ion occupied an interstitial site midway between two adjacent Li^+ vacancies, i.e. midway between the two atoms labelled A in figure 2(a). However, two Li^+ vacancies on opposite sides of a substitutional Fe^{3+} , would both compensate for all of the extra charge of Fe^{3+} and produce a site of S_4 symmetry (figure 2(b)), which is consistent with the observed spectra.

That we do not observe sites corresponding to two Li^+ vacancies occupying adjacent sites, which would be apparent from the lower symmetry, is presumably due to the electrostatic repulsion between Li^+ vacancies which separates them as far as possible in the ligand shell of Fe^{3+} , while the electrostatic attraction of the Fe^{3+} keeps them both in the ligand shell. For comparison, it is interesting that in Na_2S , which also has the antifluorite structure, Moret and Bill (1977) found only the analogous site for Gd^{3+} , charge compensated by two Na^+ vacancies.

The ionic radius of Li^+ in tetrahedral coordination with oxygen is 0.059 nm, and that of O^{2-} in eightfold coordination is 0.142 nm (Kaminskii 1975). The sum of these, 0.201 nm, is close to the Li-O distance in Li_2O of 0.2001 nm. The removal of Li^+ would allow the surrounding tetrahedron of four O^{2-} ions to move towards one another so that their centres could be as close as 0.174 nm from the centre of the tetrahedron. Fe^{3+} , with radius 0.049 nm in tetrahedral coordination (Kaminskii 1975) is smaller than Li^+ , so that its substitution for Li^+ would allow some shrinkage of the O^{2-} tetrahedron around Fe^{3+} , which would be encouraged by the extra positive charge; the sum of the ionic radii of Fe^{3+} and O^{2-} is 0.191 nm. Figure 3 shows that the absence of Li^+ at the vacancy would allow the Fe-O distance to decrease towards 0.191 nm, while maintaining the Li-O distance for Li^+ ions a and b at 0.201 nm, by a decrease in the angle θ .

For Fe-O equal to 0.191 nm, $\theta = 52.4^\circ$. Further decrease of θ would be limited when the distance between the two oxygen ions labelled A in figure 2(b) is 0.284 nm, twice the ionic radius, which for Fe-O of 0.191 nm gives $\theta = 48^\circ$; but for Fe-O of 0.200 nm it gives $\theta = 42.5^\circ$.

To a first approximation, one would expect the crystal field at the Fe^{3+} site to be dominated by the four O^{2-} ligands. At undistorted lattice positions this would lead to a cubic crystal field:

$$H_c = B_4^0 O_4^0 + B_4^4 O_4^4$$

with

$$B_4^4 = 5B_4^0.$$

However, one would expect some change in the angle θ , which would both change the ratio B_4^4/B_4^0 and introduce a term $B_2^0 O_2^0$. For a point charge model one would expect

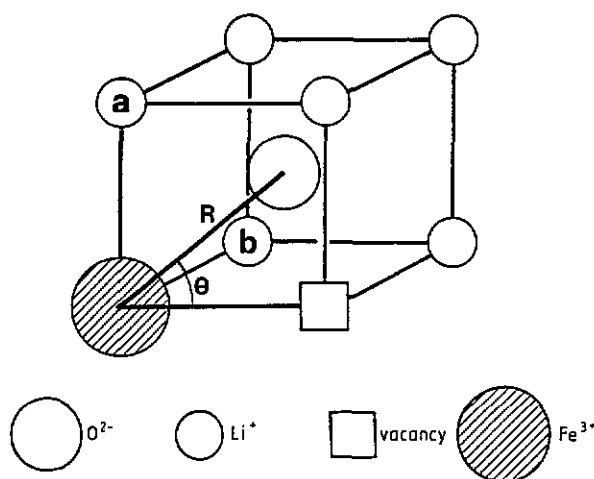


Figure 3. A detail of figure 2(b) showing the parameters for ligand positions relative to Fe^{3+} .

a similar contribution to B_2^0 from the four nearest Li^+ ions and the two Li^+ vacancies. However, it is well known that the point charge model considerably underestimates the crystal field by ignoring the effects of overlap and covalency, which is much greater for ligands. One could therefore use the superposition model of Newman (Bradbury and Newman 1976, Newman and Ng 1989) to deduce the crystal field due to the ligands, and regard the contribution of the rest of the lattice as small.

The superposition model has been used for Fe^{3+} in oxides by Yeung (1988). This supposes that, although the crystal field can produce effects in the $S = \frac{5}{2}$ ground state only in very high order of perturbation, the spin-Hamiltonian parameters b_n^m are linear functions of the crystal field. Hence, the superposition model may also be applied to the spin-Hamiltonian parameters. Yeung gives the following intrinsic parameters derived from measurements in alkaline earth oxides, for $R_0 = 0.200$ nm:

$$\begin{aligned} \bar{b}_2 &= -0.1522(48) \text{ cm}^{-1} & t_2 &= 16 \\ \bar{b}_4 &= +0.00099(8) \text{ cm}^{-1} & t_4 &= 16. \end{aligned}$$

The spin-Hamiltonian parameters for Li_2O , for four ligands at distance R and at angle θ in figure 3, may be calculated using:

$$b_n^m = \sum_i K_n^m(\theta_i, \phi_i) \bar{b}_n(R_i)$$

where

$$\bar{b}_n(R_i) = \bar{b}_n(0.200) \times (0.200/R_i)^{t_n}$$

and the sum is taken over the four ligands. The values of $K_n^m(\theta, \phi)$ are given by Newman and Ng (1989), and using these, and assuming that all four ligands are at the same distance R , gives:

$$\begin{aligned} b_2^0 &= 2(3 \cos^2 \theta - 1) \bar{b}_2(R) \\ b_4^0 &= \frac{1}{2}(35 \cos^4 \theta - 30 \cos^2 \theta + 3) \bar{b}_4(R) \\ b_4^4 &= -\frac{35}{2} \sin^4 \theta \bar{b}_4(R). \end{aligned}$$

For an undistorted tetrahedron, $R = 0.200$ nm and $\theta = 54.7^\circ$, for which the calculated parameters are:

$$b_2^0 = 0 \quad b_4^0 = -15.4 \quad b_4^4/b_4^0 = 5.0$$

where here and below we express b_n^m in units of 10^{-4} cm $^{-1}$. Both the measured large negative value of b_2^0 , and the smaller measured value of b_4^4/b_4^0 , indicate that θ is less than 54.7° , as one would expect from the likely atomic displacements discussed above. For changes of θ between 54.7° and 45° the value of K_4^0 does not change much, so the experimental value of $b_4^0 = -27(3)$ shows that R is smaller than 0.200 nm, which is expected, as discussed above. As the measured values of b_2^0 and b_4^0 are more precise than b_4^4/b_4^0 , the values of R and θ which give the measured values of the former parameters were calculated, giving

$$R = 0.194 \text{ nm} \quad \theta = 49.0^\circ$$

for which

$$b_2^0 = -1455 \quad b_4^0 = -27 \quad b_4^4/b_2^0 = 3.31.$$

The value of b_4^4/b_4^0 is in good accord with our measured value, and the numerical values of R and θ are intermediate between the extremes of an undistorted lattice and the greatest possible distortion discussed above. They correspond to a separation between the centres of the oxygen ions, labelled A in figure 2(b), of 0.292 nm, a considerable distortion from the separation of 0.327 nm in the undistorted lattice.

The largest contribution to the crystal field from more distant ions would come from the four Li^+ ions in the perpendicular plane (two of which are labelled a and b in figure 3) at a distance of 0.231 nm in an undistorted lattice. Their contribution would lead to an increase in the value of b_4^4/b_4^0 , and of $|b_4^0|$, but to a decrease in the value of $|b_2^0|$. Hence, the contribution from the four O^{2-} ligands would have to change in the opposite directions, corresponding to an increase in R and a decrease in θ . However, if at the distance of the Li^+ ions, the point charge model is used, the contribution of these ions would be only a few percent of the total crystal field, so the changes this would make to our analysis would be small.

Hence, we conclude that the application of the superposition model to our proposed structure of the Fe^{3+} site gives a satisfactory account of the spin-Hamiltonian parameters.

7. Discussion

The appearance of up to 100 ppm Fe^{3+} , after irradiation and heat treatment, raises the question of what form the iron takes in the crystal as grown.

EPR of Fe^+ ($3d^7$) has been observed in one cubic material with monovalent cations in octahedral symmetry, NaF, with $g = 4.344$ (Bleaney and Hayes 1957); it has also been observed in MgO (Orton 1959). In tetrahedral symmetry the ground state of Fe^+ would be a Γ_2 orbital singlet with $S = \frac{3}{2}$, like Cr^{2+} ($3d^3$) in an octahedral symmetry, with a g value greater than 2.0036 . For example EPR has been observed at $g = 2.248$ for Co^{2+} , isoelectronic with Fe^+ , in ZnS (Ham *et al* 1960). No such spectrum has been observed in Li_2O , suggesting that Fe^+ is not present in our crystals.

If Fe^{2+} were present in the crystal, one should consider why no EPR spectrum attributable to Fe^{2+} has been observed. The EPR of Fe^{2+} has been reported in octahedral symmetry in MgO (Low and Weger 1960) and NaF (Hall *et al* 1963), with $g = 3.428$. In tetrahedral symmetry the Γ_3 , $S = 2$, ground state is split into five equally spaced levels, whose separation depends upon the spin-spin and spin-orbit coupling and the magnitude of the crystal field; it is $10\text{--}15\text{ cm}^{-1}$ for Fe^{2+} in materials like ZnS, CdTe and $MgAl_2O_4$ (Slack *et al* 1966 and 1967). EPR has never been observed in such a system, but it would be expected only within the two triplet states at $g = 1$. This is what one would expect if Fe^{2+} were incorporated at undistorted sites in Li_2O . A measurement at ~ 9 GHz showed no evidence of EPR at $g = 1$. If Fe^{2+} were charge compensated by a neighbouring Li^+ vacancy, one would expect a site of C_{2v} symmetry (like figure 2(a)) for which the crystal field would leave an orbital singlet lowest; so one would expect, as for Cr^{2+} ($3d^4$) in $CrSO_4 \cdot 5H_2O$, a system with $S = 2$, and a g -value somewhat less than 2 (Ono *et al* 1954). The line at $g = 2.003$ cannot be attributed to such a system because for $S = 2$ there is no line at $B = h\nu/g\mu_B$. Abragam and Bleaney (1970) gives expressions (equation (7.86)) for the spin-Hamiltonian parameters appropriate to Fe^{2+} in a distorted tetrahedral environment. A calculation of the crystal field for a single Li^+ vacancy, based on the superposition model, gives a ground state for the single d-electron in the second half of the shell which is almost pure $[|+2\rangle + |-2\rangle]^{1/2}$. Scaling from the measured zero field splitting for Cr^{2+} in $CrSO_4 \cdot 5H_2O$ using typical spin-orbit and cubic crystal field parameters (table 7.3 of Abragam and Bleaney) leads to a zero field splitting for Fe^{2+} of about 4 cm^{-1} . This suggests that the reason why EPR from Fe^{2+} at such a site has not been observed in our crystals, is because the fine structure separation is larger than the microwave quantum.

These considerations suggest that the majority of the iron is incorporated into the crystal as grown in the form of Fe^{2+} whose EPR is not observed; and our measurements show that a small fraction of it is incorporated as Fe^{3+} at sites associated with other impurities which distort the local symmetry but which are not affected by x-irradiation or heating.

X-irradiation presumably generates holes and electrons which migrate through the lattice. Some holes get trapped at Fe^{2+} to form the site where Fe^{3+} is associated with two Li^+ vacancies, and the centre with $g = 2.003$ may arise from trapped electrons. However, the majority of holes must be trapped at a site we do not observe, possibly because it has greater line width than either the electron centre or that of Fe^{3+} . The spectrum near $g = 2$ is quite crowded with lines, so that a much wider line might go undetected.

Heating the crystal then presumably allows Li^+ vacancies, holes and electrons, to move. The holes recombine with the electron centre, so rendering its EPR unobservable, and also become trapped at Fe^{3+} sites to form the Fe^{3+} site we observe.

Apart from the low concentration of Fe^{3+} sites present in the crystal as grown, which do not appear to be affected by irradiation or heat treatment, the only Fe^{3+} site detected is the tetragonal site with two Li^+ vacancies. This suggests that Fe^{2+} only traps an electron when it is associated with two vacancies, and that when two vacancies are associated with Fe^{2+} (or Fe^{3+}), the linear arrangement is the only one formed.

We suggest that the iron incorporated as Fe^{2+} in the crystal as grown is associated with a neighbouring Li^+ vacancy for charge compensation. A small proportion, $\sim 5\%$, has second Li^+ vacancy in a tetragonal site. These sites are able to trap holes, even

when the sample is irradiated at 4.2 K, to form the Fe^{3+} site we observe. Heating to 500 °C allows Li^+ to diffuse away from the site opposite to the vacancy adjacent to Fe^{2+} , when a hole may be trapped at the site to form the large concentration of Fe^{3+} sites we observe after heat treatment.

That the crystal increases in weight when heated in air, and that it develops a white powdery surface layer, suggest that mobile Li^+ ions diffuse to the surface to react with oxygen atoms. This in turn suggests that the material as grown is lithium rich. If this extra lithium were in the form of interstitial Li^0 atoms, their EPR would be observable near $g = 2$ with characteristic ^7Li hyperfine structure. It seems unlikely that the extra lithium would be incorporated interstitially as either Li^+ or Li^- , so it seems likely that the crystals as grown have considerable concentration of oxygen vacancies, presumably charge-compensated by trapped holes. A large concentration of O^{2-} vacancies with two spin paired trapped electrons might account for the strong absorption in the UV of the crystals as grown. It would make it likely that x-irradiation would generate F centres, one unpaired electron trapped at an O^{2-} vacancy. After heat treatment, the concentration of O^{2-} vacancies is greatly decreased.

The nature of the centre $g = 2.003$ is not known. By comparison with the F centre in MgO (Wertz *et al* 1957), an electron trapped at an O^{2-} vacancy might be expected to have an extensive wavefunction with large transferred hyperfine interaction with neighbouring ^7Li nuclei, and hence a large line width. Even if it were relatively tightly bound to O^{2-} , one would expect that transferred hyperfine interaction with 8 ligands at 0.200 nm would produce a significantly larger line width than that of Fe^{3+} due to four ligands at 0.231 nm. The similar line width to that found in the Fe^{3+} spectrum suggests a substitutional site such as Mg^+ or Ca^+ : the weak hyperfine structure from the odd isotopes would probably not have been observed for ^{25}Mg , and would certainly not be for ^{43}Ca .

8. Conclusion

EPR has been observed for two centres in Li_2O after x-irradiation and annealing: (a) Fe^{3+} charge compensated by two adjacent Li^+ vacancies in a tetragonal site, which appears to be stable; and (b) an electron, with $g = 2.003(1)$, trapped at an unknown site which may be reversibly created by x-irradiation and destroyed by annealing.

Acknowledgments

We are grateful to Dr F Pratt for assistance with the optical absorption measurements, to Mr A O'Connell for some EPR measurements and Professor W Hayes for discussion and advice.

References

- Abragam A and Bleaney B 1970 *Electron Paramagnetic Resonance in Transition Ions* (Oxford: Oxford University Press)
- Akiyama M, Ando K and Oishi Y 1980 *J. Nucl. Sci. Technol.* **17** 154
- Baker J M and Chaplin D 1979 *J. Phys. C: Solid State Phys.* **12** L129
- Baker J M and Robinson P 1983 *Solid State Commun.* **48** 551

- Bleaney B and Hayes W 1957 *Proc. Phys. Soc. B* **70** 626
- Bradbury M I and Newman D J 1976 *Chem. Phys. Lett.* **1** 44
- Farley T W D, Hayes W, Hull S, Ward R, Hutchings M T and Alba M 1988 *Solid State Ion.* **28-30** 189
- Hall T P P, Hayes W, Stevenson R W H and Wilkins J 1963 *J. Chem. Phys.* **38** 1977
- Ham F S, Ludwig G W, Watkins G D and Woodbury H H 1960 *Phys. Rev. Lett.* **5** 468
- Kaminskii A A 1975 *Laser Crystals* (Moscow: Nauka) p 256
- Low W and Weger M 1960 *Phys. Rev.* **118** 1119
- Moret J M and Bill H 1977 *Phys. Status Solidi a* **41** 163
- Newman D G and Ng B 1989 *Rep. Prog. Phys.* **52** 699
- Ohno H, Konishi S, Nagasaki T, Katsuta H and Watanabe H 1985 *J. Nucl. Mater.* **133/134** 181
- Ono K, Koide S, Sekimaya H and Abe H 1954 *Phys. Rev.* **96** 38
- Orton J W 1959 *Rep. Prog. Phys.* **22** 204
- Shindo I, Kimura S, Noda K, Kurasawa T and Nasu S 1979 *J. Nucl. Mater.* **79** 418
- Slack G A, Ham F S and Chrenko R M 1966 *Phys. Rev.* **152** 376
- Slack G A, Roberts S and Ham F S 1967 *Phys. Rev.* **155** 170
- Stevens K W H 1952 *Proc. Phys. Soc. A* **65** 209
- Wertz J E, Austins P, Weeks R A and Silsbee R H 1957 *Phys. Rev.* **107** 1535
- Yeung Y Y 1988 *J. Phys. C: Solid State Phys.* **21** 2453